SL-MD Note 203
PS/PA/Note 96-05 (MD)
3rd, 5th and 10th October 1995
SPS

Observation and improvement of the transverse characteristics of the proton beam delivered by CPS in Continuous Transfer mode

G. Arduini, J. Boillot, R. Cappi, G. Ferioli, M. Martini and K. Metzmacher

Keywords: Injection, Beam instrumentation, SPS machine, Transverse

Summary

Two split foils in TT10 have been equipped with wide band readout electronics in order to measure the evolution of the position of the beam centroid of the proton beam during the continuous transfer from CPS to SPS. Vertical excursions have been observed during the spill with a maximum amplitude of about 20 mm (peak-to-peak). No relevant displacement has been observed in the horizontal plane. An almost complete cancellation of the above phenomenon has been achieved in three steps:

- adjustment of the timing of the kick provided by the Emittance Reduction Dipole (ERD1) in TT2 acting on the last (5th) PS turn;
- increase of the strength of the above kick;
- addition of a second kick provided by a spare ERD (ERD2) to adjust independently the 4th and 5th PS turns.

This resulted in a reduction of the average vertical emittance of the injected beam of up to 21% and in an improvement of the injection efficiency in the SPS ring of up to 3%.

Index

1. Introduction

The high intensity proton beam is delivered to SPS in two batches, each about 10.5 μs long, extracted horizontally in 5 PS turns. Extraction is obtained by setting the horizontal tune Q_H in PS to 6.25 and driving the beam against an electrostatic septum by means of a set of slow (DHZ and BHZ in Fig. 1) and fast (BFA in Fig. 1) bumper dipoles. The fast bumpers generate a horizontal oscillation in the orbit, between BFA21 and BFA9, superimposed to the local bumps created by the slow bumpers at the electrostatic septum (SES31 in Fig. 1) and magnetic septum (SMH16 in Fig. 1) positions. The circulating beam is therefore cut in the horizontal phase plane according to the scheme represented in Fig. 2. The intensity profile of the extracted beam is adjusted by acting on the current functions driving the fast bumpers in the machine (staircase adjustment - see Fig. 3).

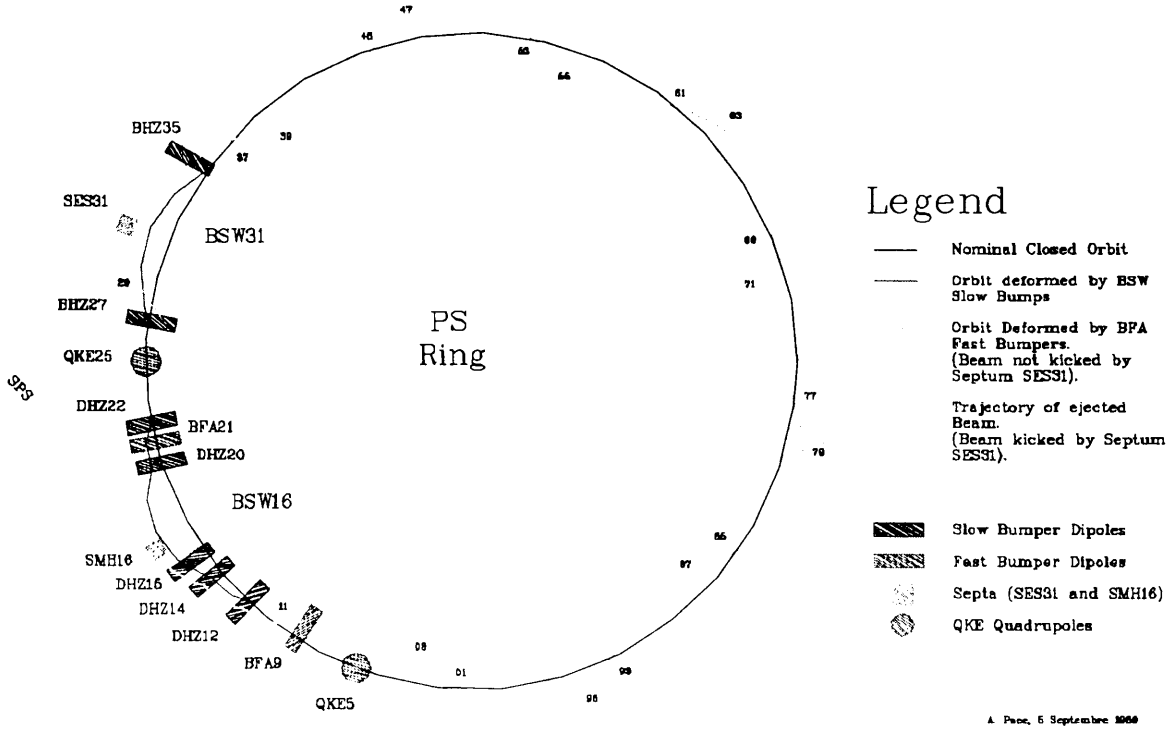

Fig. 1. Extraction elements used in PS for the Continuous Transfer method: location of the extraction bumps.

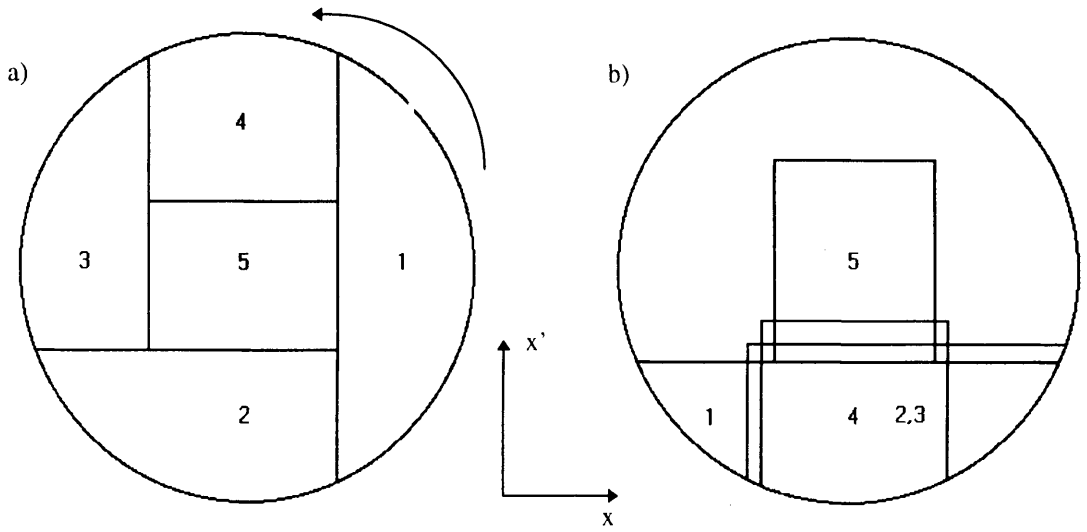

Fig. 2. Schematic representation in the horizontal phase plane (normalized coordinates) of the Continuous Transfer process: a) the "slices" in which the circulating beam is cut at the electrostatic septum SES31, b) the extracted beam at the exit of the extraction magnetic septum SMH16.

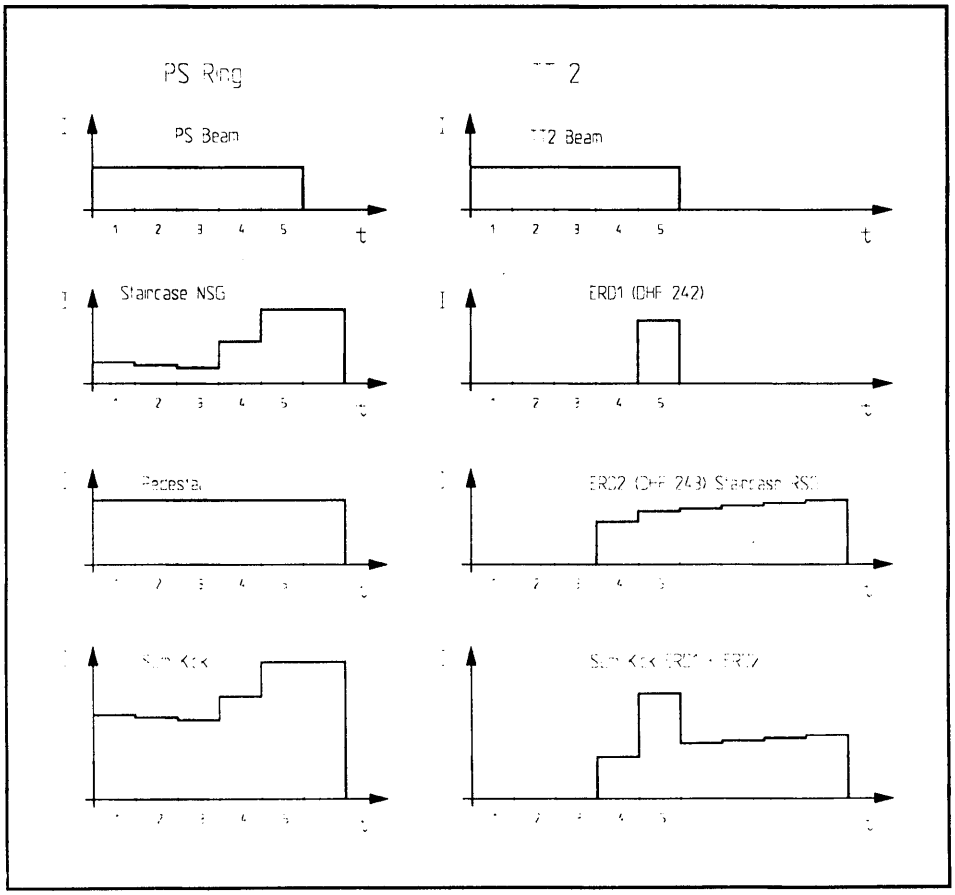

Fig. 3. Extraction elements used in PS for the Continuous Transfer method: typical current functions of the PS shaving bumpers and the TT2 Emittance Reduction Dipoles. The combined use of the two TT2 ERDs done in the last MD session (see Section 5.3) is also shown in the last two plots. NSG = New Staircase Generator, RSG = Reserve Staircase Generator.

The particles constituting the core of the circulating beam are extracted in the last turn and present themselves at the septum with a different average horizontal angle as compared to that of the particles extracted in the previous turns. In order to minimize the horizontal emittance of the beam, integrated over the 5 PS turns, a fast electromagnetic kicker (Emittance Reduction Dipole - ERD1 - see Table 1), located in TT2, provides a horizontal kick in correspondence of the 5th PS turn to compensate for the different extraction conditions with respect to the other 4 turns. The parameters that can be used to optimize the horizontal transverse structure of the extracted beam are the kick strength and the time at which the kicker is fired.

Magnet data		ERD 1 (DHF 242)	ERD 2 (DHF 243)
Aperture width	(mm)	158	158
Aperture height	(mm)	53.5	53.5
Length	(mm)	625	600
Coil windings		2	1
∫Bdl max.	(Gauss m)	147	202
∫Bdl/I	(Gauss m/A)	0.147	0.1408
∫Bdl/PFN voltage	(Gauss m/kV)	4.45	5.46
Rise time (10-90)%	(ns)	510	510
Generator data		ERD	RSG
No. of steps		1 × 2.3 μs	5 × 2.2 μs
PFN voltage max.	(kV)	33	37
I max.	(A)	500	1435

Tab. 1. Basic characteristics of the Emittance Reduction Dipoles.

As a result of the extraction process above described the vertical emittance of the beam is larger than the horizontal. In order to cope with the SPS transverse acceptance, which is smaller in the vertical plane, an emittance exchange insertion consisting of three skew quadrupoles is placed at the beginning of the transfer line TT10.

Any error in the adjustment of the ERD parameters produces drifts of the beam centroid in the SPS vertical plane during the spill and therefore a blow-up of the vertical emittance of the injected beam, with a consequent reduction of the transmission efficiency.

2. Instrumentation description

The beam centroid position is measured by two split foils in TT10 near the injection point (BSPH1029 and BSPV1029). At the present time, only one electronic chain is available, therefore after a check of the horizontal evolution of the beam centroid during the spill (which did not show any relevant structure) the vertical position of the center was considered in detail.

In order to perform the measurements, the secondary emission currents emitted by the foils, are amplified by two fast current-to-voltage converters installed close to the detector. The amplitudes of the signals A and B are digitized and recorded at a frequency of 10 MHz (i.e. approximately 100 points per PS turn) by a 8-bit FADC.

The *(A-B)/(A+B)* and the *A+B* signals, related to the beam centroid position (see Section 4) and intensity during the spill, respectively, can be displayed on a X-terminal and saved for off-line analysis. For the 1996 run both BSPH1029 and BSPV1029 will be equipped with the above described electronics and the sampling frequency will be increased to 30 MHz. In this way the structure of the 4 PSB turns for each PS turn should be clearly visible.

3. Preliminary tests

Preliminary tests of the measurement system were performed with the split foil BSPH1029 (horizontal plane) where the readout electronics was initially installed. Possible sources of noise were determined and their relevance quantified. A clear correlation between the SPS injection kicker status and the noise measured in the split foil signals was observed (see Figs. 4a, 4b, 5a and 5b).

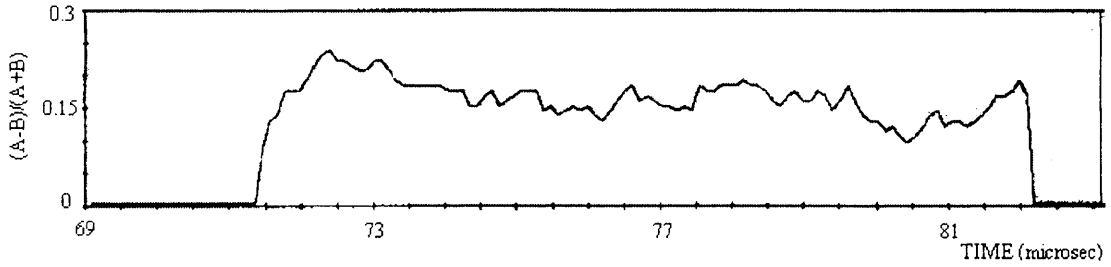

Fig. 4a. Temporal evolution of the *(A-B)/(A+B)* signal from BSPH1029 (related to the beam centroid position) during the spill (1st batch 22/06/1995 - 11:04:06). The SPS injection kicker was OFF during the measurement. The origin of the time scale is arbitrary.

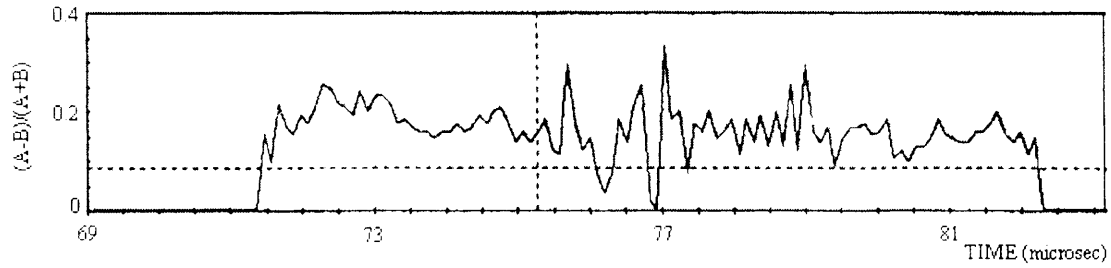

Fig. 4b. Temporal evolution of the *(A-B)/(A+B)* signal from BSPH1029 (related to the beam centroid position) during the spill (1st batch 22/06/1995 - 10:59:49). The SPS injection kicker was ON during the measurement. The origin of the time scale is arbitrary.

The noise appears with a reproducible time structure when the kicker is ON: an oscillation appearing approximately 4 μs after the beginning of the spill, lasting approximately 3 μs and noticeable in both the intensity and beam position profiles. The peak-to-peak amplitude of this oscillation correspond to 2 - 3 mm according to the

calibration curve described in the following section. An analogous behaviour has been observed with the split foil BSPV1029.

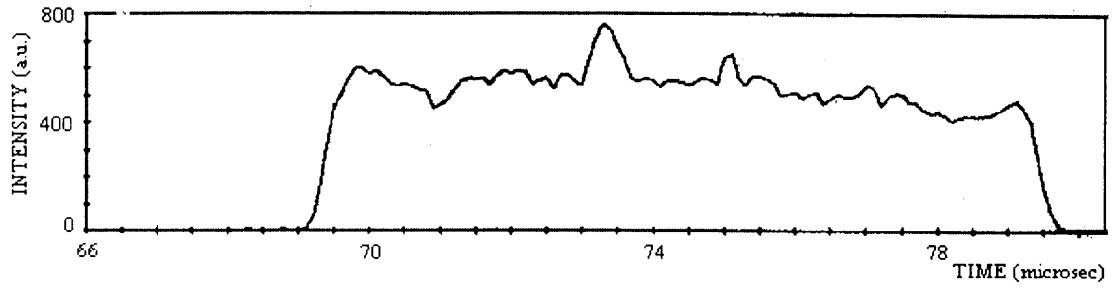

Fig. 5a. Intensity profile (arbitrary units) of the 1st batch (22/06/1995 10:59:49). The SPS injection kicker was OFF during the measurement.

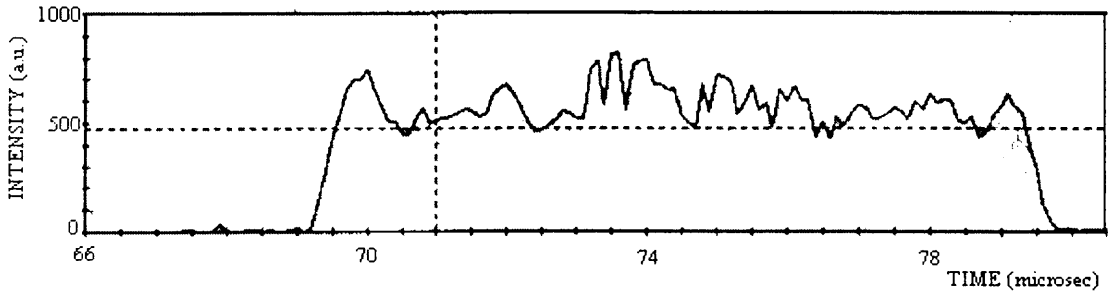

Fig. 5b. Intensity profile (arbitrary units) of the 1st batch (22/06/1995 - 11:04:06). The SPS injection kicker was ON during the measurement.

4. Calibration curve

A theoretical calibration curve (see Fig. 6) representing the displacement y of the centroid of the beam (normalized to the r.m.s. size σ of the beam at the split foil position) as a function of the amplitude of the signals A and B measured in the two foils[1] has been calculated according to the following expression

$$\frac{A-B}{A+B} = \frac{1}{\sqrt{2\pi}} \int_{-1/\sigma}^{1/\sigma} \exp\left(-\frac{z^2}{2}\right) dz$$

valid for the assumption of a gaussian profile.

A preliminary test has been performed to verify the accuracy of the proposed calibration curve. In this respect a displacement of the vertical beam position at the spilt foil BSPV1029 has been produced by means of an upstream vertical corrector

[1] We assume that A and B are the signals measured in the foils covering the positive and negative coordinate ranges, respectively.

(MDIV1027 consisting of two dipoles powered in series: MDIV102702 and MDIV102703) and the vertical displacement has been measured.

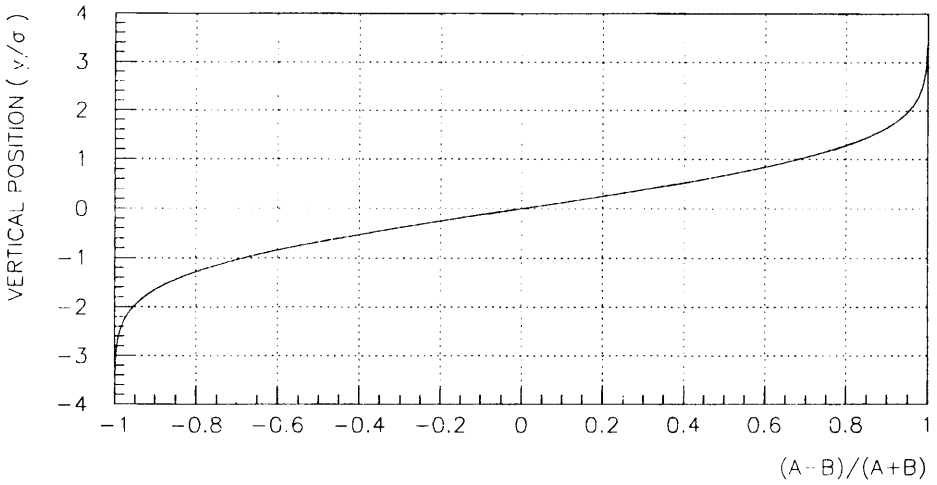

Fig. 6. Calibration curve providing the displacement of the centroid of the beam (normalized to the r.m.s. size of the beam at the split foil position) as a function of the ratio *(A-B)/(A+B)* of the signals *A* and *B* recorded from the two foils.

The r.m.s. vertical size of the beam at the foil has been calculated from that measured at the SEM grid BSG1029 in TT10, taking into account the values of the β functions at the two points (the vertical dispersion at the two points is negligible). All the machine development studies here described were performed during physics, therefore only three series of measurements (each consisting of three) with the SPS injection kicker ON were taken not to disturb operation. The trims ΔI = 0.0, -0.220275, -0.44055 A, in the current I supplied to the magnets MDIV102702 and MDIV102703, were applied. The average of the three profiles measured for each value of the current has been taken, the differences of the mean profiles corresponding to different kicks have been considered and the mean and r.m.s. values of the distribution of each difference along the spill calculated. The results are shown Table 2. No dependance of the mean on the width of the averaging window has been noticed within the quoted errors. The measured displacement is linearly dependent on the kick, as expected, within the errors of the measurement.

Kick - MDIV1027 (mrad)	Calculated displacement (MAD) BSPV1029 (mm)	Measured displacement BSPV1029 (mm)	
		I batch	II batch
- 0.0443	- 4.3	- 3.0 ± 0.7	- 2.8 ± 1.0
- 0.0887	- 8.6	- 5.8 ± 1.1	- 6 ± 1.6

Tab. 2. Comparison of the calculated and measured displacement of the average vertical beam position at BSPV1029 produced by a kick provided by the corrector MDIV1027.

The nominal magnetic field provided by the MDIV1027 dipoles for a currrent of 3.2 A is 0.047 T and the magnetic length is L = 0.32 m [1]. The kicks corresponding to the above current trims have been calculated assuming that:

- the iron in the return yoke is not saturated when the magnet is operated at 3.2 A and therefore the magnetic field varies linearly with the current;
- the bending power provided by the two magnets is exactly the sum of the bending power of the individual dipoles.

In that case the kick $\Delta\theta$ provided by the two magnets in series is given by:

$$\Delta\theta(rad) = 2 \times 0.2997925 \frac{\Delta B(T) L(m)}{p(GeV/c)} \tag{1}$$

where

$$\Delta B(T) = 0.047 \frac{\Delta I(A)}{3.2} \tag{2}$$

and ΔB is the variation in the magnetic field in each dipole produced by the trim ΔI, p is the momentum of the proton beam (14 GeV/c).

The expected displacement of the beam centroid has been calculated with MAD (see Table 2). The linear fit of the data points ($\Delta\theta$, Δx_m), where Δx_m is the measured displacement, gives:

$$\Delta x_m(mm) = (66.3 \pm 95.2) \times \Delta\theta(mrad)$$
$$\Delta x_m(mm) = (65.9 \pm 198.6) \times \Delta\theta(mrad)$$

for the first and second batch, to be compared with the calculated values:

$$\Delta x\ (mm) = 97.0 \times \Delta\theta(mrad).$$

The measured coefficient 66.2 ± 85.8 mm/mrad (average of the values found for the two batches) is approximately 32% lower than the calculated one, even if the two values are compatible as a consequence of the large error in the measurement. The possible concurrent origins of the discrepancy between the average of the measured coefficient and the calculated one could be:

- the uncertainties in the coefficient relating kick strength and current for each magnet MDIV1027;
- the non linear superposition of the transverse component of the magnetic field. The distance between the yokes of the two dipoles is in fact only 150 mm (i.e. less than twice the magnet gap that is 88 mm wide), therefore a variation of the distribution of the magnetic field of each dipole, due to the presence of the yoke of the other, is expected;
- the uncertainty in the values of the β functions at the BSG1029 and BSPV1029 positions;

- the small number of measurements and the noise in the position measurement due to the SPS injection kicker, which are responsible of the large errors associated with the measurements and with the fitted parameters.

5. Beam observations in TT10

Figs. 4a and 4b show that the oscillations of the beam centroid in the horizontal plane are negligible, these correspond to a peak-to-peak oscillation of 1 mm, according to the calibration curve displayed in Fig. 6. This amplitude is smaller than the signal induced by the SPS injection kicker and is definitely negligible as compared to the amplitude of the oscillations observed in the vertical plane (see below).

5.1 MD session on 3rd October 1995

Figs. 7 and 8 show typical vertical position and intensity profiles observed in TT10 before the machine development session. The corresponding relevant beam parameters are summarized in Table 3.

ε_H [π mm mrad][2]		ε_V [π mm mrad][2]		M_H[3]		M_V[3]	
1st batch	2nd batch	1st batch	2nd batch	1st batch	2nd batch	1st batch	2nd batch
2.53 ± 0.26	2.59 ± 0.25	1.358 ± 0.022	1.345 ± 0.022	1.68±0.08	1.62±0.06	1.68±0.01	1.68±0.01
Intensity in TT10 [10^{13} protons per batch]					2.1 - 2.3		
Extraction losses at PS [%]					10		
SPS Injection efficiency [%]					98 - 99		
SPS transmission efficiency @ 440 GeV [%]					93 - 94		

Tab. 3. Relevant beam parameters at the beginning of the MD session (03/10/95). Emittances and blow-up factors are an average of 5 measurements.

In order to avoid wrong position readings due to noise or low intensities observable at the beginning and at the end of the spill a threshold has been fixed so that only the position of the beam for intensities higher than 10% of the peak intensity are calculated and displayed.

The two opposite peaks observable in the position of the beam (see Fig. 7) at the beginning and at the end of the spill occur as a consequence of the finite rise-time and fall-time of the magnetic field in the extraction fast bumpers in the PS (a few hundreds ns). The five turn structure in the batch is visible in the beam position and in the intensity profiles, in particular a large fluctuation of the beam position between the 4th and 5th turn (about 20 mm peak-to-peak) has been detected and traced to be a consequence of a non optimum timing of the ERD1 kick.

---

[2] The error in the emittance value takes into account only the statistical error in the estimate of the r.m.s. size of the profiles measured at the grids.

[3] The blow-up factor M represents the expected emittance blow-up of the beam injected in the SPS resulting from the mismatch between the optical functions measured in one point (BSG1027) of the transfer line TT10 and their values calculated with MAD assuming a perfect matching at the injection point.

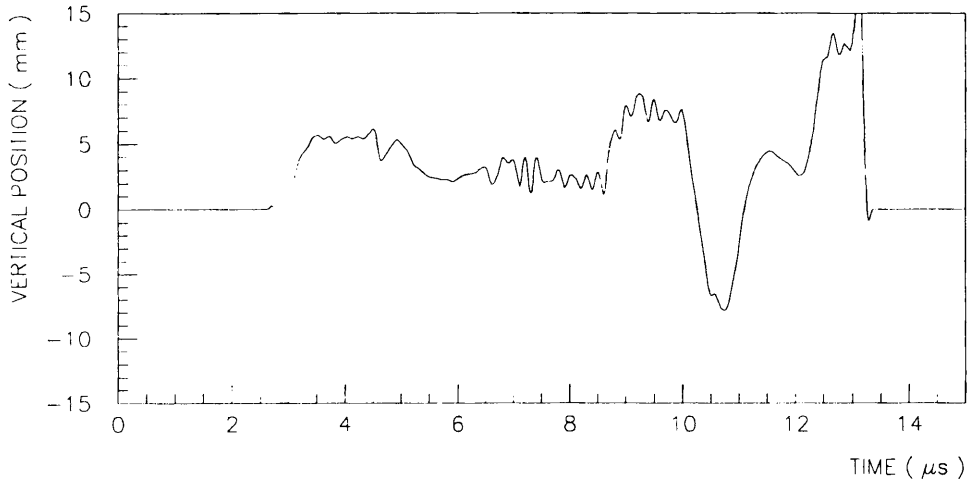

Fig. 7. Temporal evolution of the vertical position of the beam centroid during the spill (2nd batch - 03/10/1995 - 16:37:44). The average r.m.s. vertical beam size at BSPV1029 was σ_V = 6.933 mm.

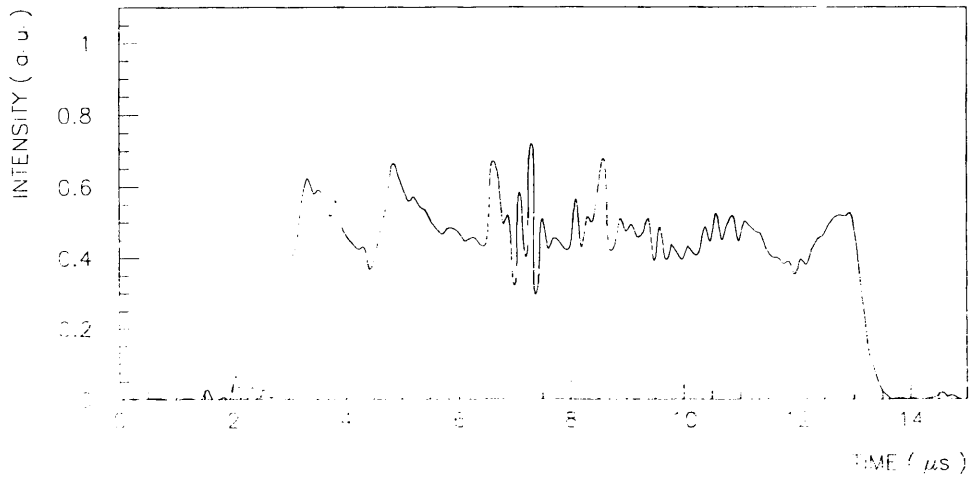

Fig. 8. Intensity profile of the 2nd batch (03/10/1995 - 16:37:44).

The adjustment of the ERD1 timing (delayed by 735 ns) resulted in a reduction of a factor 4 of the oscillation of the vertical beam position during the spill (5 mm peak-to-peak). The observed profiles for the vertical position and the intensity are illustrated in Figs. 9 and 10, respectively, while the relevant beam parameters after the ERD adjustment are presented in Table 4.

A reduction of the vertical emittance by about 21% was observed in TT10 and a new record on transmission efficiency (96.3%) at high intensity (4.162 x 10^{13} ppp at 440 GeV) was established.

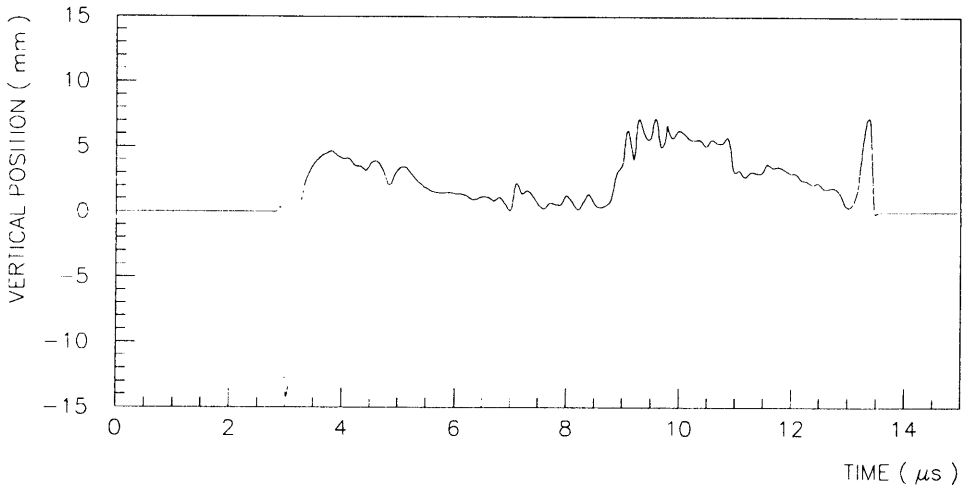

Fig. 9. Temporal evolution of the vertical position of the beam centroid during the spill (2nd batch - 03/10/1995 - 20:10:24). The average r.m.s. vertical beam size at BSPV1029 was σ_V = 6.353 mm.

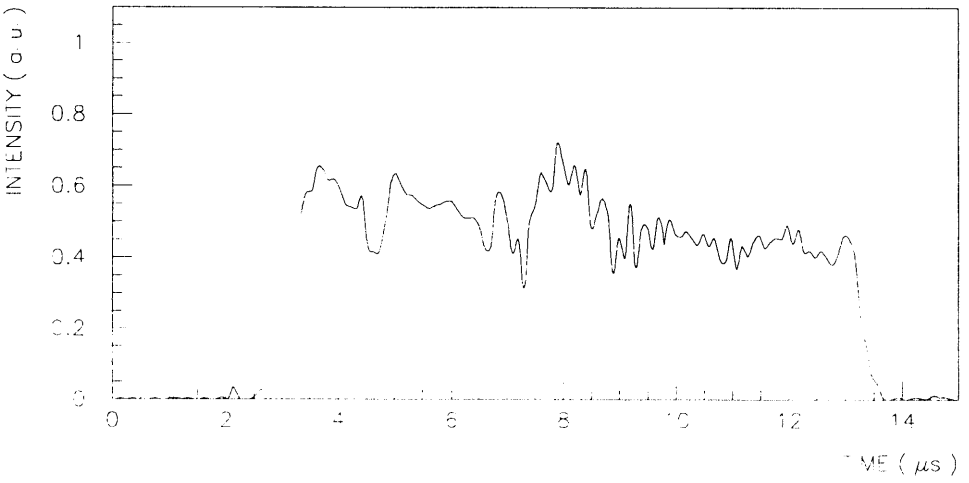

Fig. 10. Intensity profile of the 2nd batch (03/10/1995 - 20:10:24).

ε_H [π mm mrad]		ε_V [π mm mrad]		M_H		M_V	
1st batch	2nd batch	1st batch	2nd batch	1st batch	2nd batch	1st batch	2nd batch
2.48 ± 0.24	2.50 ± 0.23	1.070 ± 0.010	1.055 ± 0.009	1.70±0.13	1.65±0.07	1.92±0.08	1.91±0.07
Intensity in TT10 [10^{13} protons per batch]						2.1 - 2.3	
Extraction losses at PS [%]						10.7	
SPS Injection efficiency [%]						> 99	
SPS transmission efficiency @ 440 GeV [%]						95 - 96	

Tab. 4. Relevant beam parameters at the end of the MD session (03/10/95). Emittances and blow-up factors are an average of 6 measurements.

5.2 MD session on 5th October 1995

A second MD session was arranged to verify the dependence of the 5 turn alignment of the beam centroid on the ERD1 kick strength. Table 5 summarizes the main beam parameters at the beginning of the MD session.

ε_H [π mm mrad]		ε_V [π mm mrad]		M_H		M_V	
1st batch	2nd batch	1st batch	2nd batch	1st batch	2nd batch	1st batch	2nd batch
2.38 ± 0.25	2.40 ± 0.24	1.053 ± 0.017	1.052 ± 0.016	1.81±0.09	1.8±0.13	2.35±0.05	2.34±0.05

Intensity in TT10 [10^{13} protons per batch]	2.0 - 2.1
Extraction losses at PS [%]	11.1
SPS Injection efficiency [%]	97
SPS transmission efficiency @ 440 GeV [%]	92

Tab. 5. Relevant beam parameters at the beginning of the MD session (05/10/95). Emittances and blow-up factors are an average of 7 measurements.

No evident reason was found for the worse vertical profile of the beam (see Fig. 11), apparently no parameter regulating the behaviour of the extraction elements had been changed since the end of the previous MD session. The smaller vertical (and horizontal) emittance observed at the beginning of the MD notwithstanding the poorer vertical alignment of the 5 turns (with respect to that measured in the previous session - see Fig. 9) can be partially explained with the lower intensity delivered by CPS (about 10% lower as compared to the previous MD session).

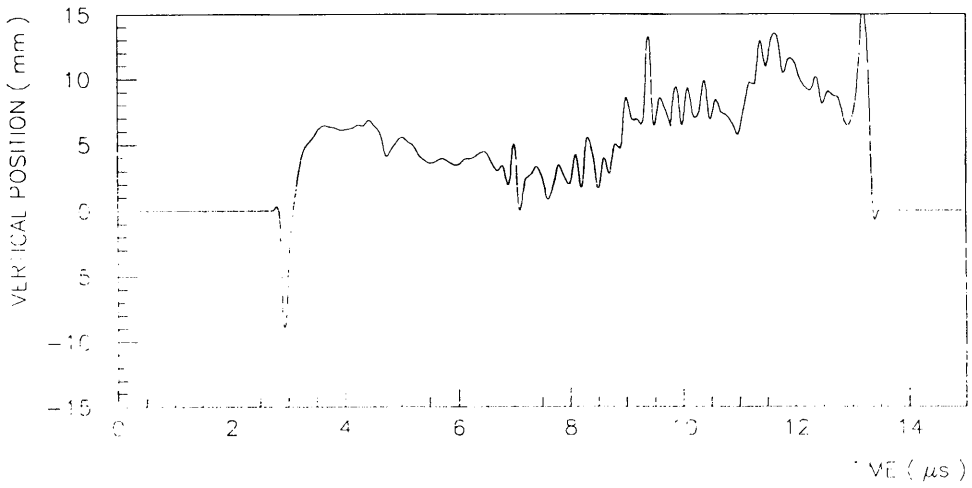

Fig. 11. Temporal evolution of the vertical position of the beam centroid during the spill (2nd batch - 05/10/1995 - 08:56:51). The average r.m.s. vertical beam size at BSPV1029 was σ_V = 7.206 mm.

The strong structure observed in the intensity profile of the spill and the tail observed after the 5th PS turn are symptoms of the non optimum conditions of the delivered beam and are likely responsible for the lower transmission efficiency in the SPS, as compared to the previous MD session. These were traced back to PSB instabilities that could not be eliminated during the MD.

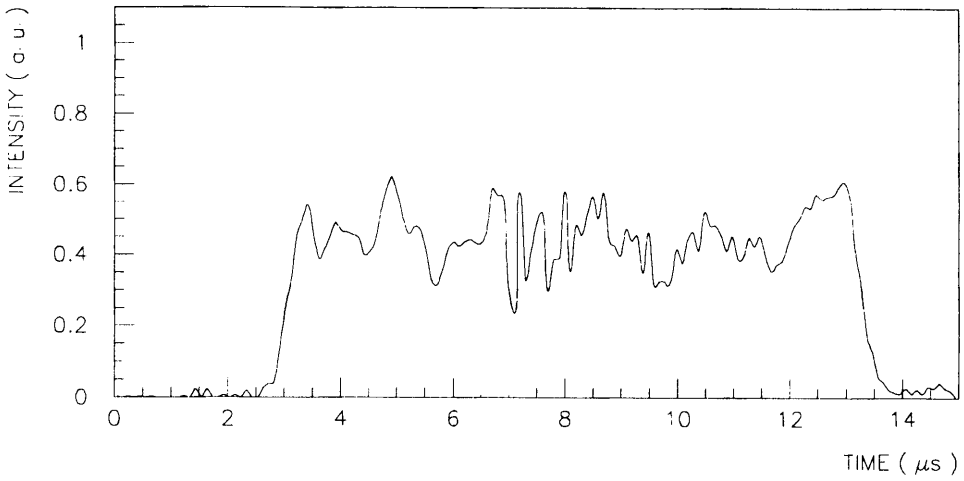

Fig. 12. Intensity profile of the 2nd batch (05/10/1995 - 08:56:51).

A first attempt of aligning the vertical position of the centroid of the beam during the spill was done by increasing the ERD1 kick strength to the maximum voltage that could be provided by the power supply (i.e. 37.5 kV). The effect of this operation on the position and intensity profiles is shown in Figs. 13 and 14.

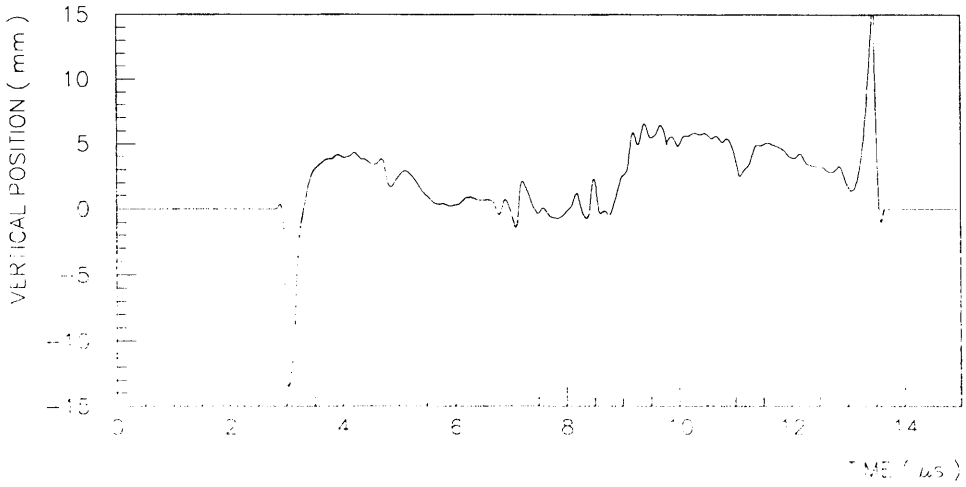

Fig. 13. Temporal evolution of the vertical position of the beam centroid during the spill (2nd batch - 05/10/1995 - 16:36:33). The average r.m.s. vertical beam size at BSPV1029 was σ_V = 7.505 mm.

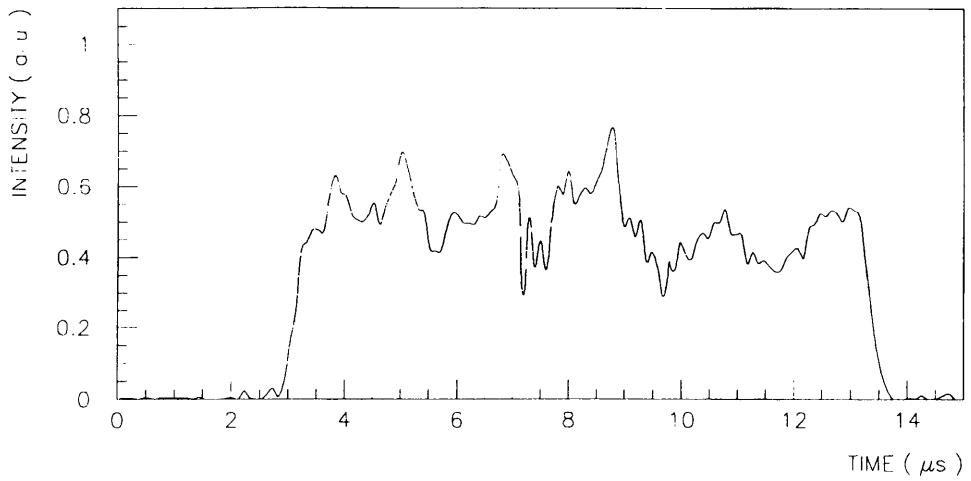

Fig. 14. Intensity profile of the 2nd batch (05/10/1995 - 16:36:33).

Following the above test the kick strength was reduced to 31 kV which is the maximum safe operation limit for the ERD1 power supply and the above profiles have been obtained (see Figs. 15 and 16).

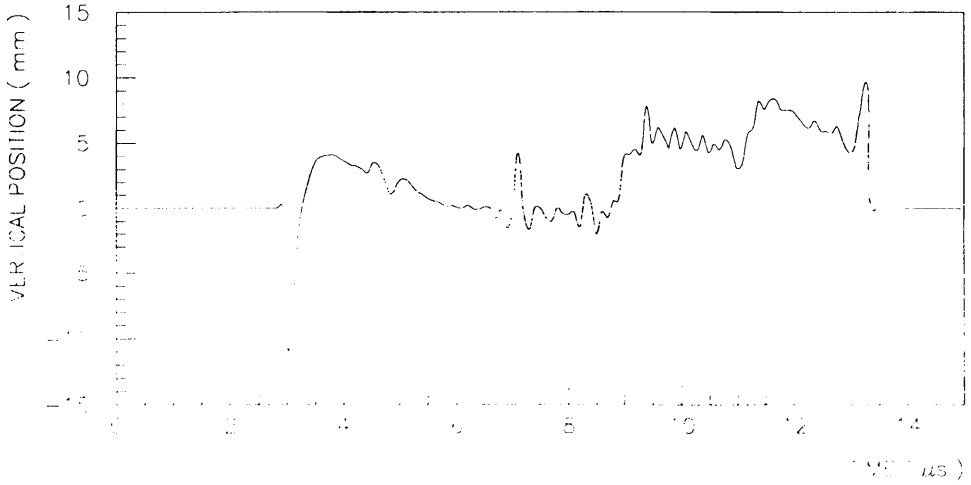

Fig. 15. Temporal evolution of the vertical position of the beam centroid during the spill (2nd batch - 05/10/1995 - 16:44:18). The average r.m.s. vertical beam size at BSPV1029 was σ_V = 7.505 mm.

The peak-to-peak amplitude of the oscillation of the vertical beam position could not be reduced below 8 mm. The main beam parameters after this final adjustment are listed in Table 6.

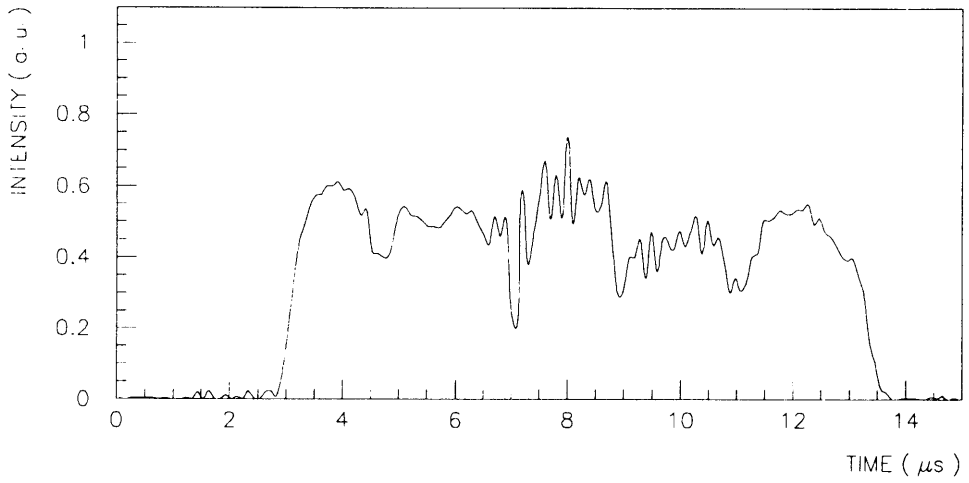

Fig. 16. Intensity profile of the 2nd batch (05/10/1995 - 16:44:18).

ε_H [π mm mrad]		ε_V [π mm mrad]		M_H		M_V	
1st batch	2nd batch	1st batch	2nd batch	1st batch	2nd batch	1st batch	2nd batch
2.38 ± 0.24	2.59 ± 0.22	0.962 ± 0.016	1.018 ± 0.014	1.9 ± 0.2	1.73±0.02	2.8 ± 0.1	2.63±0.05
Intensity in TT10 [10^{13} protons per batch]						2.0 - 2.1	
Extraction losses at PS [%]						11.4	
SPS Injection efficiency [%]						97.5	
SPS transmission efficiency @ 440 GeV [%]						92	

Tab. 6. Relevant beam parameters at the end of the MD session (05/10/95). Emittances and blow-up factors are an average of 9 measurements.

A reduction of the vertical emittance by 6% was obtained at the end of the MD session but the improvement of the injection efficiency was limited (0.5%) and no improvement in the overall transmission efficiency was noticed. PSB instabilities, responsible for the poor intensity structure of the spill, are likely the origin of the non-optimum transmission efficiency.

5.3 MD session on 10th October 1995

As a result of the previous MD sessions it could be concluded that:

- the maximum *safe* ERD1 kick strength is not sufficient to compensate for the different average extraction angle of the particles during the 5th turn (see Figs. 9 and 15);
- full alignment of the vertical beam centroid position during the spill is not possible even if running the ERD power supply above the operational limit as it acts only on the fifth turn, while a different vertical position is also observed between the first three turns and the fourth one (see Figs. 9, 13, 15).

It was therefore decided to use a second ERD (ERD2) placed just after ERD1 (exactly 50 mrad in the horizontal phase advance) to provide a kick, both to the 4th and 5th

turns, superimposed to the kick provided by ERD1. This is equivalent to impart to the extracted beam in TT2 a modulated horizontal kick in the form of a two-step staircase signal, in which the timing and the amplitude of the two steps can be adjusted independently (see Fig. 3).

For the second time the spill characteristics at the beginning of the MD session were found to be worse than those recorded at the end of the previous MD session, but again without any apparent reason. Nevertheless it must be remembered that this last MD session followed a restart after two days without beam because of a vacuum leak in the Linac. The position and intensity profiles are shown in Figs. 17 and 18 while the beam parameters are listed in Table 7.

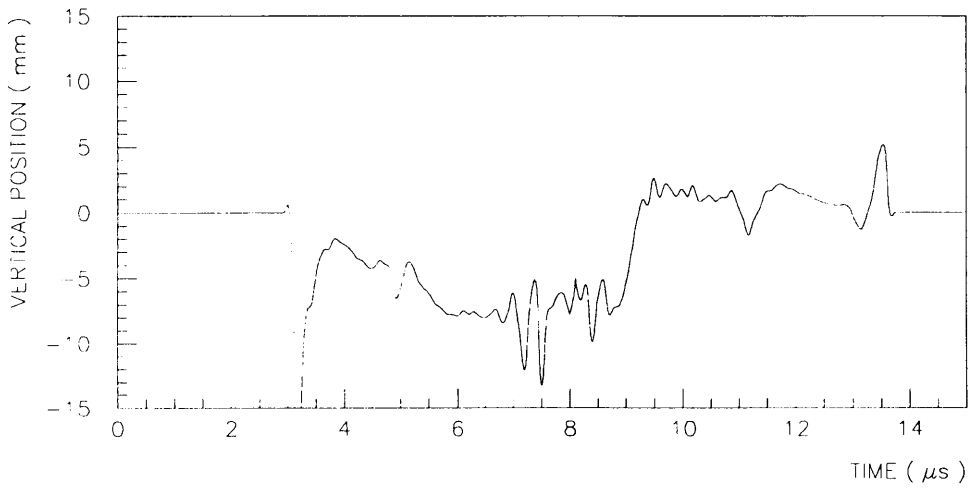

Fig. 17. Temporal evolution of the vertical position of the beam centroid during the spill (2nd batch - 10/10/1995 - 07:25:12). The average r.m.s. vertical beam size at BSPV1029 was σ_V = 7.997 mm.

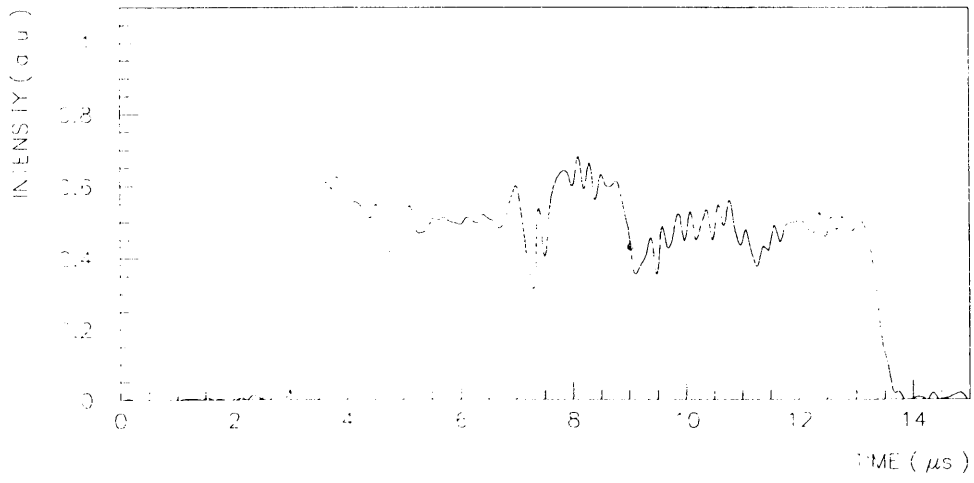

Fig. 18. Intensity profile of the 2nd batch (10/10/1995 - 07:25:12).

ε_H [π mm mrad]		ε_V [π mm mrad]		M_H		M_V	
1st batch	2nd batch	1st batch	2nd batch	1st batch	2nd batch	1st batch	2nd batch
2.47 ± 0.29	2.55 ± 0.29	1.246 ± 0.014	1.248 ± 0.013	1.86±0.1	1.86±0.15	2.45±0.01	2.45±0.03

Intensity in TT10 [10^{13} protons per batch]	2.0 - 2.2
Extraction losses at PS [%]	12 - 12.5
SPS Injection efficiency [%]	96
SPS transmission efficiency @ 440 GeV [%]	89

Tab. 7. Relevant beam parameters at the beginning of the MD session (10/10/95). Emittances and blow-up factors are an average of 6 measurements.

The timing of ERD1 was delayed by 105 ns with respect to the value set for the previous sessions, while the time advance of ERD2 with respect to ERD1 was about 2.1 μs (i.e. one PS turn). After the adjustment of the ERD staircase the beam parameters listed in Table 8 could be obtained, while the corresponding position and intensity profiles are presented in Figs. 19 and 20, respectively.

ε_H [π mm mrad]		ε_V [π mm mrad]		M_H		M_V	
1st batch	2nd batch	1st batch	2nd batch	1st batch	2nd batch	1st batch	2nd batch
2.43 ± 0.25	2.52 ± 0.25	1.166 ± 0.014	1.163 ± 0.011	1.83±0.08	1.76±0.03	2.17±0.01	2.17±0.02

Intensity in TT10 [10^{13} protons per batch]	2.0 - 2.2
Extraction losses at PS [%]	11.6
SPS Injection efficiency [%]	99
SPS transmission efficiency @ 440 GeV [%]	92

Tab. 8. Relevant beam parameters at the end of the MD session (10/10/95). Emittances and blow-up factors are an average of 7 measurements.

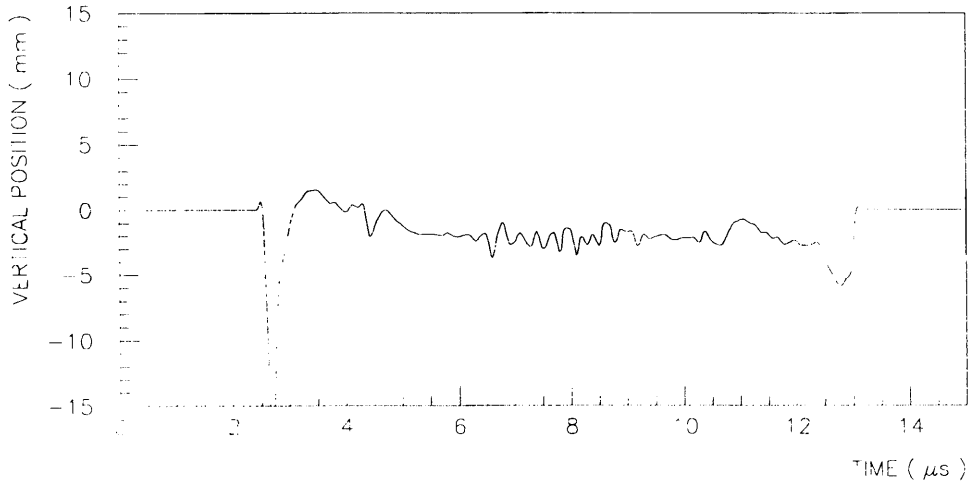

Fig. 19. Temporal evolution of the vertical position of the beam centroid during the spill (2nd batch - 10/10/1995 - 15:03:53). The average r.m.s. vertical beam size at BSPV1029 was σ_V = 7.151 mm.

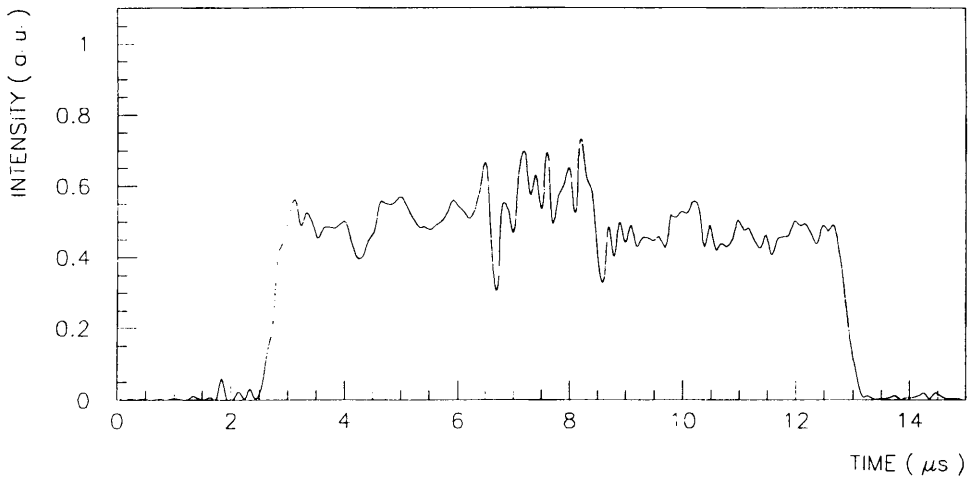

Fig. 20. Intensity profile of the 2nd batch (10/10/1995 - 15:03:53).

The vertical emittance of the injected beam was reduced by 7% and injection and overall transmission efficiencies in the SPS were increased by 3% as a result of the described actions.

The emittance measurements performed at the end of the adjustment showed an asymmetric vertical profile of the extracted beam (see Fig. 21). This feature, never noticed before, is not completely unexpected if one takes into account the extraction mechanism. This asymmetric profile could have been hidden by the vertical motion of the beam centroid along the spill, before the ERD adjustment. This asymmetry was not observed after the preliminary adjustments performed in the first session, though the amplitude of this motion was already strongly reduced, but started to appear after the second session (Fig. 22) and further increased in the last session when poorer transmission efficiencies were observed in the SPS. In both cases the asymmetric profile could be clearly observed only after the ERD adjustment.

An increase of the vertical mismatch factor has also been remarked during the adjustment procedure and in particular, in the first two sessions an increase was always observed after the ERD adjustment. This seems to indicate that the beam is matched when the vertical position of the beam centroid oscillates (and therefore the average vertical emittance is blown-up) but not when the vertical positions of the beam centroid of the five PS turns are aligned (and no emittance blow-up should be expected).

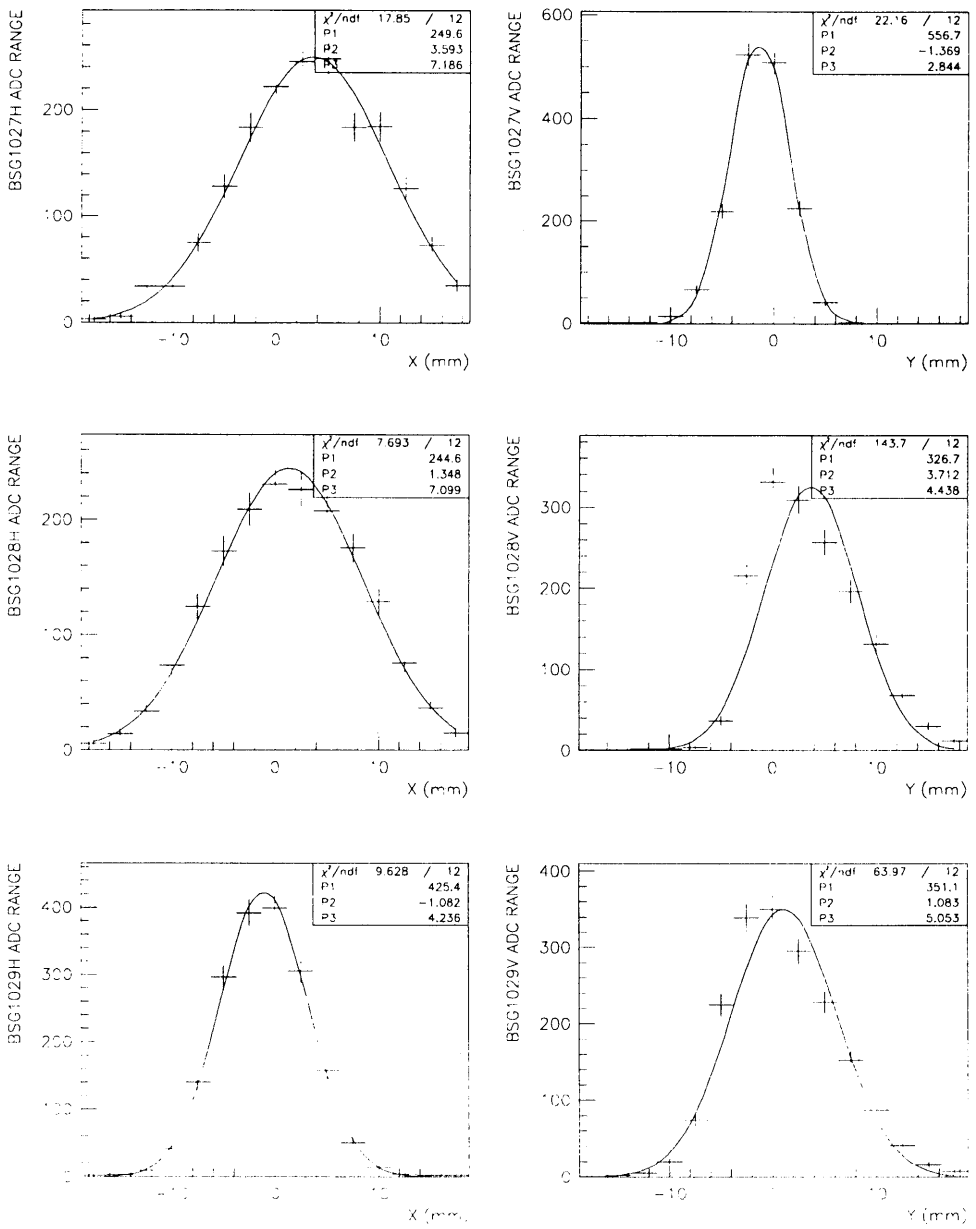

Fig. 21.Horizontal and vertical profiles of the beam at the SEM grids BSG1027/1028/1029 in TT10 (2^{nd} batch - 10/10/1995 - 15:30).

It is also worth to report two other actions taken by the SPS operation crews during the period in which the MD sessions took place, in order to minimize instabilities at the transition:

1. increase of the *vertical* strength of the machine octupoles used for Landau damping. This increase, started from the end of July 1995 when a gradual reduction of the vertical emittance of the proton beam from 1.5 to 1.3 π mm mrad was measured, was enhanced during the second half of September and continued during the MD (Fig. 23);

2. adjustment of the RF feedback delay for the travelling wave cavities used for proton acceleration were required.

The occurrence of the instabilities at transition could be related to the reduction of the vertical emittance of the beam and therefore to the increased space charge density, nevertheless Linac and PSB instabilities, which could also be the causes of such instabilities, were also signalled during the MD period.

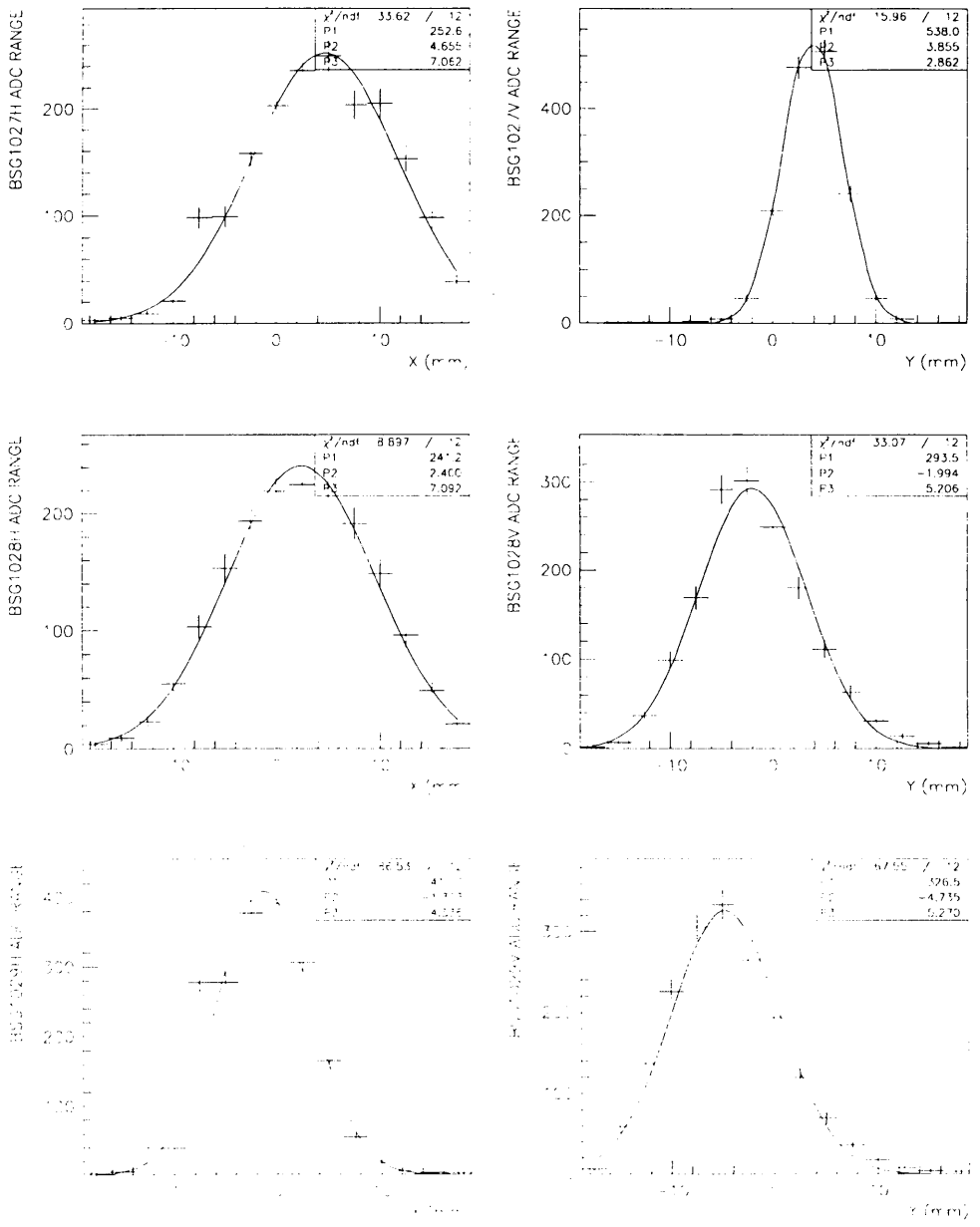

Fig. 22.Horizontal and vertical profiles of the beam at the SEM grids BSG1027/1028/1029 in TT10 (2^{nd} batch - 05/10/1995 - 17:00).

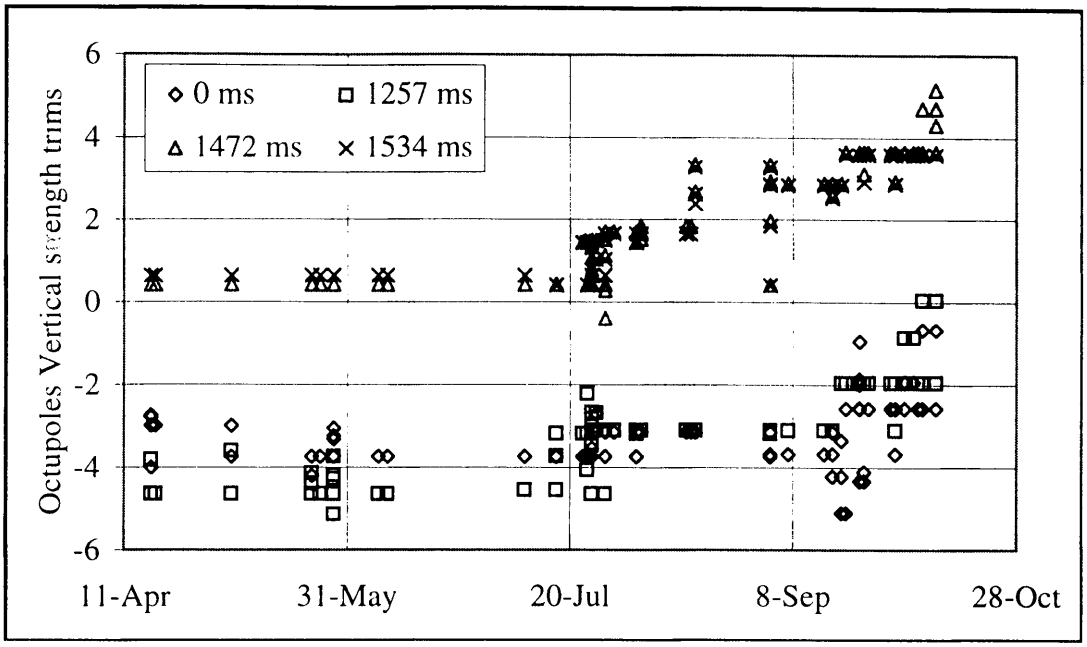

Fig. 23.Trims in the vertical strength of the octupoles used for Landau damping. Only the trims performed during operation are presented.

6. Summary and conclusions

The intensity and beam centroid position profiles along the spill of the beam delivered by CPS in Continuous Transfer mode have been measured by means of wide-band readout electronics installed on the horizontal split foil BSPH1029 and afterwards on the vertical split foil BSPV1029. A theoretical calibration curve and the measurement of the beam size in the SEM grid BSG1029 in TT10 have been used to determine the amplitude of the beam centroid oscillations. The accuracy of the proposed calibration curve has been checked by kicking the beam vertically by a known amount and comparing the measured displacement with the calculated one. This test has evidenced the linearity of the response in a range of 8 mm and a good agreement between expected and measured values, taking into account the uncertainties in the optics of the transfer line and in the integrated field provided by the corrector magnets.

The main source of noise in the measurement has been identified in the SPS injection kicker, nevertheless the amplitude of the noise signal has a reproducible structure and is largely smaller than the oscillation observed in the vertical plane.

No relevant oscillation of the beam centroid has been detected in the horizontal plane while an oscillation of about 20 mm (peak-to-peak) has been observed between the 4th and 5th PS turns. A strong attenuation of the vertical excursion of the beam position along the spill has been achieved in the following steps:

- adjustment of the timing of the kick provided ERD1 in TT2 acting on the last (5th) PS turn;
- increase of the strength of the above kick;
- addition of a second kick provided by a spare ERD (ERD2) to adjust independently the 4th and 5th PS turns.

A reduction of the average vertical emittance of the injected beam of up to 21% and an improvement of the injection efficiency in the SPS ring of up to 3% have been achieved in this way.

By the beginning of the 1996 run both ERD1 and ERD2 will be available and will have remotely controlled amplitude. Both BSPH1029 and BSPV1029 will be equipped with the fast readout electronics with an enhanced sampling frequency (30 MHz).

A complete calibration of both the horizontal and vertical beam position measurements will be performed in a wider range (± 15 mm) and with a larger number of points. The uncertainty in the function relating the current provided to the corrector magnet and the kick provided to the beam should be eliminated by measuring the beam displacement in the SEM grids used for the emittance measurement. The focussing strength of the quadrupoles of the transfer line TT10 are in fact well known, as well as the spacing between the strips of the SEM grids.

The appearance of asymmetric tails in the vertical profile of the beam should be confirmed and possible correlations with transmission efficiency in the SPS and with any extraction parameter in the PS should be further investigated. Matching of the TT10 transfer line optics with that one of the SPS ring at the injection point should be verified once the vertical beam position profile along the spill is adjusted. The possible outbreak of instabilities at low energy and at the transition as a function of the vertical emittance (varied by acting on the ERD staircase) should be studied at high intensity (about 2.1×10^{13} ppb) with stable injection conditions.

7. Acknowledgments

We would like to thank J.J. Gras for providing a preliminary version of the software used to display the signals from the split foils on a X-terminal in the Prevessin and Meyrin Control Rooms and to store the measured data for off-line analysis.
We also express our thanks to L. Sermeus for making ready and operational the Reserve Staircase Generator (RSG) required for pulsing ERD2.

8. References

[1] J. Riche, 'Proposition pour les mesures de controle des dipoles de correction', Note 300-MA/Int-73-3, 6th June 1973.